Check for updates

Nanoscale disintegration kinetics of mesoglobules in aqueous poly(*N*-isopropylacrylamide) solutions revealed by small-angle neutron scattering and pressure jumps†

Bart-Jan Niebuur,‡[a] Leonardo Chiappisi, [iD][b,c] Florian A. Jung,[a] Xiaohan Zhang,[a] Alfons Schulte [iD] *[d] and Christine M. Papadakis [iD] *[a]

Identification and control of the disintegration mechanism of polymer nanoparticles are essential for applications in transport and release including polymer delivery systems. Structural changes during the disintegration of poly(*N*-isopropylacrylamide) (PNIPAM) mesoglobules in aqueous solution are studied *in situ* and in real time using kinetic small-angle neutron scattering with a time resolution of 50 ms. Simultaneously length scales between 1 and 100 nm are resolved. By initiating phase separation through fast pressure jumps across the coexistence line, 3 wt% PNIPAM solutions are rapidly brought into the one-phase state. Starting at the same temperature (35.1 °C) and pressure (17 MPa) the target pressure is varied over the range 25–48 MPa, allowing to systematically alter the osmotic pressure of the solvent within the mesoglobules. Initially, the mesoglobules have a radius of gyration of about 80 nm and contain a small amount of water. Two disintegration mechanisms are identified: (i) for target pressures close to the coexistence line, single polymers are released from the surface of the mesoglobules, and the mesoglobules decrease in size, which takes ~30 s. (ii) For target pressures more distant from the coexistence line, the mesoglobules are swollen by water, and subsequently the chains become more and more loosely associated. In this case, disintegration proceeds within less than 10 s, controlled by the osmotic pressure of the solvent.

Introduction

Naturally occurring and man-made assemblies of nanostructures from (bio)macromolecules are ubiquitous. The disintegration mechanisms and their kinetics are of importance for applications as diverse as the processing of polymer powders,[1,2] the separation of polymer blends,[3] the disintegration of microplastics in living systems[4] and of polymeric

delivery systems after drug release,[5–9] and the dissolution of polymer scaffolds used in tissue engineering.[10] A structural understanding of these processes is essential to improve their design and, thereby, to enhance their functionality. In this article, we address the fundamental mechanisms that are involved in the disintegration of polymeric nanoparticles.

In contrast to particles composed of small molecules or atoms, the disintegration of particles from macromolecules, such as cellulose[11,12] or proteins[13,14] are governed by more complex mechanisms, in that not only diffusion, but also disentanglement processes are vital.[5] Early work on the disintegration of macroscopic, glassy particles from homopolymers revealed that, due to solvent diffusion into the polymer grain, a swollen polymer layer forms at its surface.[4,15–17] With time, its interfaces with the solvent matrix and the glassy inner part of the particle move away from each other. From the swollen layer, the polymers disentangle and reach the solvent. In atomistic simulations of a surface of short polystyrene chains in toluene, it was found that a thin swollen layer forms almost instantaneously.[18] The chains from this layer become solvated, while the toluene front moves deeper into the polymer matrix.[18] The time needed to turn a solvent-free polymer grain into a dilute solution was found to be limited by the life-time of the swollen polymer

[a]*Physik-Department, Fachgebiet Physik weicher Materie, Technische Universität München, James-Franck-Straße 1, 85748 Garching, Germany*
[b]*Institut Laue-Langevin, Soft Matter Science and Support group, 71, Avenue des Martyrs, 38042 Grenoble, France*
[c]*Technische Universität Berlin, Stranski Laboratorium für Physikalische und Theoretische Chemie, Institut für Chemie, Straße des 17. Juni 124, Sekr TC7, 10623 Berlin, Germany*
[d]*Department of Physics and College of Optics and Photonics, University of Central Florida, 4111 Libra Drive, Orlando, FL 32816-2385, USA.*
E-mail: alfons.schulte@ucf.edu

†Electronic supplementary information (ESI) available: Comparison of pre-jump states. Analysis of SANS data. Intermediate pressure jumps. See DOI: 10.1039/d1nr02859f
‡Present address: INM - Leibniz Institute for New Materials, Campus D2 2, 66123 Saarbrücken, Germany.

layer.[19] The swelling process is driven by the osmotic pressure of the solvent as well as by its gel permeability. Once the polymer concentration in the swollen layer has reached the overlap concentration, the polymers are released into the solution by convection. For grains in the millimetre size range, the disintegration process takes several minutes.[17]

While previous studies have addressed large, solvent-free polymer grains on slow timescales, there is a lack of experiments on water-dispersible polymer nanoparticles including those relevant for biomedical applications. Here, the microscopic size of the mesoglobules is particularly relevant as well as the presence of a certain fraction of water inside. Aqueous dispersions of mesoglobules formed by the thermoresponsive polymer poly(N-isopropylacrylamide) (PNIPAM) may serve as a model system to investigate the effect of the osmotic pressure of the solvent on the disintegration of small polymeric nanoparticles. In aqueous solution, PNIPAM features lower critical solution temperature (LCST) behavior with an LCST of ∼32 °C.[20] Upon heating through the cloud point, the chains strongly dehydrate[21–24] and collapse.[25,26] The collapsed PNIPAM chains form mesoglobules, i.e., long-lived aggregates typically having sizes between tens of nanometers to several micrometers.[27–30] The origin of their long lifetime is their rigid shell which hinders their coalescence.[30] In turbidity and dynamic light scattering experiments during slow cooling of an aqueous dispersion of PNIPAM mesoglobules, two disintegration steps were identified: an initial swelling process, which was related to the entanglements of the polymer, and the subsequent release of single polymers.[31] When the number of polymer entanglements in the mesoglobules was reduced, only the release of single polymers was observed.

The coexistence line of PNIPAM solutions may not only be traversed by a change in temperature, but also by changing pressure. Rapid pressure changes on the millisecond timescale enable the study of the early stages of mesoglobule disintegration. Moreover, varying the target pressure allows to alter the osmotic pressure of the solvent inside the mesoglobules, one of the key factors for disintegration.[19] Kinetic small-angle neutron scattering (SANS) offers the possibility to track particle disintegration with excellent spatial and temporal resolution and over large time and length scales: the accessible time range spans from tens of milliseconds to thousands of seconds, i.e., over 4 decades, which allows monitoring the time up to full disintegration of the mesoglobules. The range of momentum transfers in reciprocal space corresponds to length scales from the sub-nanometer regime to hundreds of nanometers. Therefore, not only the particle sizes, but also their inner and surface structure as well as concentration fluctuations in the polymer solution are measurable during mesoglobule disintegration. Our previous studies of the inverse processes, namely chain collapse and mesoglobule formation following a sudden change of a PNIPAM solution from the one-phase to the two-phase state, have demonstrated the potential of this approach.[32,33]

In the present work, we exploit pressure jump initiated SANS kinetics over 4 decades in time to investigate the disinte-gration of mesoglobules, as the solutions rapidly turn from the two-phase to the one-phase state. With increasing range of the jump, osmotic pressure and water content of the mesoglobules become important.

Experimental

Materials

Poly(N-isopropylacrylamide) (PNIPAM) with M_n = 36 kg mol^{-1} and Đ = 1.26 was purchased from Sigma-Aldrich. PNIPAM was dissolved in D$_2$O (Deutero, 99.95%) at a polymer concentration of 3 wt%, which is in the semi-dilute concentration regime.[32] The solutions were shaken for at least 48 h at room temperature.

Time-resolved small-angle neutron scattering (TR-SANS)

TR-SANS experiments were performed at the instrument D11 at the Institut Laue-Langevin (ILL), Grenoble, France, along the lines described previously.[32,33] In brief, a neutron wavelength of λ = 0.6 nm with a spread $\Delta\lambda/\lambda$ = 0.09 was selected. The measurements were performed with sample-detector distances (SDDs) of 1.5, 8.0 and 34.0 m, resulting in a range of momentum transfers, q, of 0.02–3.3 nm^{-1}, with $q = 4\pi \times \sin(\theta/2)/\lambda$ where θ is the scattering angle.

The experimental approach is illustrated in Fig. 1. We exploit the increase of the cloud point from 33.7 °C at atmospheric pressure to 35.9 °C at ∼60 MPa. At temperatures in-between, the one-phase state, where the polymers are molecularly dissolved, can be reached by an increase in pressure from the two-phase state, where a mesoglobule dispersion is present. At the temperature chosen, 35.1 °C, the coexistence line is located at 21.8 ± 2.5 MPa.[33] Pressure jumps to four target pressures were performed, starting at an initial pressure of 17 MPa to target pressures p_{target} = 25, 30, 36 or 48 MPa, respectively (Fig. 1). At this, the same set-up as described previously was used.[32,33] Before each jump, the pressure was set to 17 MPa. Then a pneumatically driven valve (PDV) between the sample cell and the pressure generator was closed, and the
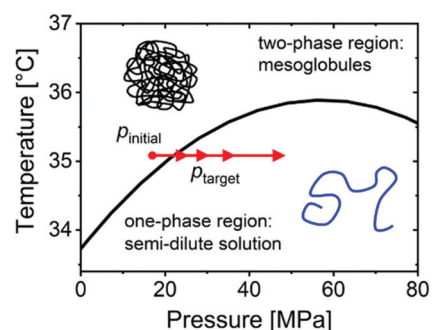

Fig. 1 Experimental scheme. The black line denotes the coexistence line between the mesoglobules dispersion and the semi-dilute solution, as determined by turbidimetry.[32] The red arrows indicate the initial pressure and the target pressures of the 4 jumps.

pressure in the external system was set to a higher value. The system was equilibrated for 5 min, and a static SANS measurement (pre-jump measurement) with a measuring time of 1 min at each SDD was carried out (a detailed description on the protocol of reaching the initial state is given in the ESI†). The pressure jumps were performed within 25 milliseconds by rapidly opening the PDV with a pulse, causing the pressure in both sections to equilibrate at p_{target} and triggering the start of the SANS data acquisition. The frame duration was 0.05 s and was successively increased after each frame by a factor of 1.1. After each pressure jump, 85 frames were recorded, resulting in a total measuring time of 1649 s. The measurements at SDD = 34 m were repeated at least 5 times for each jump and were averaged. The time resolution of the experiment is limited by the response time of the PDV and the flight time of the neutrons between the sample and the detector (<~0.05 s).

SANS data analysis

All scattering curves were fitted by the model

$$I(q) = I_{LS}(q) + I_{OZ}(q) + I_{bkg} \qquad (1)$$

where $I_{LS}(q)$ accounts for large-scale structures and the Ornstein–Zernike structure factor $I_{OZ}(q)$ describes local concentration fluctuations. An incoherent background, I_{bkg}, is added as a floating parameter and took values of 0.05–0.1 cm^{-1}. Before the jumps and during early times after the jump (up to 3.5 and 0.40 s for p_{target} = 25 MPa and 48 MPa, respectively), the Guinier–Porod form factor[34] was used for $I_{LS}(q)$ to describe the size and structure of the mesoglobules. It contains the radius of gyration of the mesoglobules, R_g, the Porod exponent m, describing the surface structure of the mesoglobules,[35,36] and an amplitude I_G (which represents their molar mass). The Ornstein–Zernike structure factor[37] is used throughout to describe local concentration fluctuations, which are due to inhomogeneities inside the mesoglobules and/or to dissolved chains. It comprises the correlation length of concentration fluctuations, ξ_{OZ}, and an amplitude I_{OZ}. At later times, remaining weak forward scattering resulting from large-scale inhomogeneities was modeled using the Porod form factor, which contains the Porod amplitude K_P and the Porod exponent m.[38] A detailed description of the data analysis is given in the ESI†.

Results and discussion

The initial state

The static SANS data recorded prior to the jumps from $p_{initial}$ = 17 MPa to p_{target} = 25 or 48 MPa are shown in the same graph as the kinetics (Fig. 2a and b). The pre-jump spectra feature a shoulder at low q values, which is due to scattering from mesoglobules. In the high-q region, a weak shoulder indicates inhomogeneities inside the mesoglobules. The curves are fitted using eqn (1) with the Guinier–Porod form factor and the Ornstein–Zernike structure factor (see the ESI† for the fits as
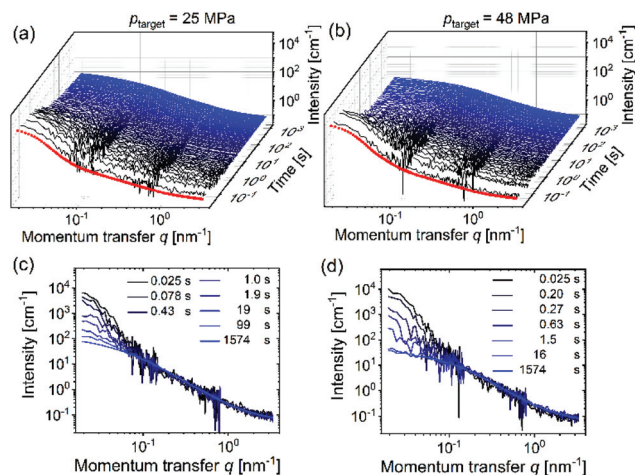

Fig. 2 Upper panels: SANS curves of the 3 wt% PNIPAM solution in D_2O after jumps from the two-phase state to the one-phase state starting at T = 35.1 °C and $p_{initial}$ = 17 MPa to p_{target} = 25 MPa (a) and p_{target} = 48 MPa (b) from short times (black curves) to long times (blue curves). Red symbols: Pre-jump scattering curves. Lower panels: Selected scattering curves obtained after the jumps to p_{target} = 25 MPa (c) and p_{target} = 48 MPa (d) at the times indicated in the graphs.

well as their individual contributions). The resulting radii of gyration of the mesoglobules amount to R_g = 71–72 nm. The Porod exponent, indicative of the surface structure of the mesoglobules, is m = 4.6 ± 0.1, pointing to a composition gradient at their surface.[35,36] As shown previously,[33] the mesoglobules have a dense PNIPAM shell, which prevents their coalescence. In addition, the shell traps water inside the mesoglobules, leading to inhomogeneities with a correlation length $\xi_{OZ} \cong 7$ nm.

Mesoglobule disintegration

Overview. The SANS scattering curves following a pressure jump are displayed in Fig. 2a and b. The essential characteristics of the kinetics are observed in jumps starting at $p_{initial}$ = 17 MPa to the smallest and the largest target pressures, p_{target} = 25 MPa (Fig. 2a and c) and 48 MPa (Fig. 2b and d), both in the one-phase region. Further jumps to two intermediate target pressures are described in the ESI†. The most prominent feature after both jumps is the decrease of the intensity of the shoulder at small q values (below 0.1 nm^{-1}) during the first few seconds. The behaviour of this shoulder, resulting from scattering at the mesoglobules, differs in both cases: for the shallowest jump, the shoulder shifts towards larger q values (Fig. 2c) during the first seconds, pointing to a size decrease of the mesoglobules. In contrast, for the deepest jump, it shifts to smaller q values (Fig. 2d), indicating that the mesoglobules grow. In both cases, the scattering intensity in the high-q region changes only weakly.

The kinetics are fitted to the same model as for the pre-jump data, taking into account the Ornstein–Zernike structure factor and the Guinier–Porod form factor at early times and the Porod form factor at late times. Excellent agreement

between the data and the fits is obtained in all cases (for examples see Fig. S2 and S3 in the ESI†). Fig. 3 displays the resulting structural parameters.

The shallowest jump. For p_{target} = 25 MPa, the Guinier amplitude I_G and the shape parameter m remain rather constant during the first 0.35 s, while R_g increases slightly from 72 to 87 nm (left column in Fig. 3). This may point to the swelling of the outer layer of the mesoglobules, in line with theoretical predictions.[18] Between 0.35 and 3.5 s, I_G decreases. This may, *a priori*, be due to the penetration of D$_2$O into the mesoglobules or by a decrease of the number and/or the volume of the mesoglobules due to the release of polymers into the solution. The simultaneous decrease of R_g to ~60 nm, however, strongly indicates that the release of polymers into the solution dominates. This scenario is supported by the decrease of m from ~4.6 to ~2.2, *i.e.*, the surface of the mesoglobules becomes increasingly rough, and the mesoglobules transform from compact particles to loose clusters of polymers. During this time period, the inhomogeneities inside the mesoglobules probed by the Ornstein–Zernike amplitude I_{OZ}, are unchanged for the first 2.0 s. The subsequent rapid decrease of I_{OZ} along with a slight decrease of ξ_{OZ} from ~6.2 to ~3.0 nm suggests that the mesoglobules become more homogeneous, possibly

because the trapped water dissolves the chains inside the mesoglobules. In addition, this contribution may include scattering from released polymers.

After 3.5 s, R_g and m have decreased to ~60 nm and ~2, and the slope of the Guinier–Porod contribution is the same as the one from the Ornstein–Zernike term at high q values. Therefore, the contributions from the mesoglobules, from their inner structure and from the polymers in solution overlap strongly and are all described by the Ornstein–Zernike structure factor. The latter is used from this time onwards, while weak forward scattering reflecting weak large-scale concentration fluctuations is accounted for by a Porod term with $m \cong 2$.[32] Except for a sharp increase 3.5 s after the jump, which we attribute to the change of fitting model, ξ_{OZ} continues the decreasing trend of R_g, until it becomes constant after ~30 s and reaches a value of 17.6 nm, which is the value of the final semi-dilute solution.[30] I_{OZ} decreases as well and becomes constant at the same time, *i.e.*, the solution becomes homogeneous, and the released polymers increasingly dominate the scattering.

Thus, for the shallow jump, we observe predominantly the formation of a diffusion layer, the release of polymers from the surface of the mesoglobules, starting after 0.35 s, and subsequently the enrichment of the surrounding aqueous matrix with polymers (bottom row of Fig. 4a). Moreover, the mesoglobules become more homogeneous because the trapped water becomes distributed. Asymptotically, a semi-dilute solution with weak large-scale inhomogeneities is reached after ~30 s, consistent with previous observations.[30]

The mechanism identified here is compatible with the release of single chains from a thin swollen surface layer.[5,10,19,31,39,40] In contrast to previous macroscopic experiments on PNIPAM mesoglobules carried out using turbidimetry and light scattering and at a low cooling rate,[31] our time-resolved SANS experiments provide not only information on the overall size of the mesoglobules, but also on their surface topology and their inner structure. Pressure jumps along with time-resolved SANS provide unprecedented time resolution in the millisecond range, which is essential to resolve the key structural changes on the micro- and nano-scales.

The deepest jump. The structural parameters obtained for the jump with p_{target} = 48 MPa are shown in Fig. 3b, d and f. After ~0.1 s, R_g starts to increase, while I_G starts to decrease, and ξ_{OZ} increases from 4.0 to 18.9 nm at 0.35 s. Afterwards, the value of R_g is so high that it cannot be resolved any more due to the limited q range, and therefore, the Porod form factor is used after this time instead of the Guinier–Porod form factor. Between 0.35 and 10 s, I_{OZ} decreases slightly, and ξ_{OZ} decreases to 11.9 nm, *i.e.*, the inner structure of the mesoglobules is nearly unchanged. Meanwhile, m decreases from ~4.6 to ~2, *i.e.*, the mesoglobules become large, loosely packed clusters. After ~10 s, ξ_{OZ} levels off at 11.0 nm. Thus, again a semi-dilute PNIPAM solution with weak large-scale inhomogeneities is reached, albeit along a different pathway.

To conclude, for the deepest pressure jump, mesoglobule disintegration is fundamentally different from the one found
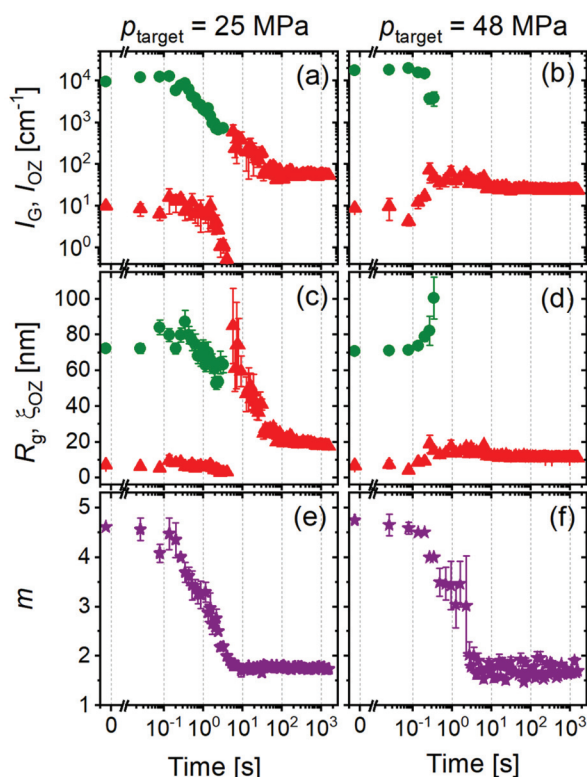

Fig. 3 Time dependence of the structural parameters from fitting the SANS data for the jumps to the target pressures indicated above the graphs. (a, b) Guinier amplitude I_G (green circles) and Ornstein–Zernike amplitude I_{OZ} (red triangles). (c, d) Radius of gyration of the mesoglobules, R_g (green circles) and correlation length of concentration fluctuations, ξ_{OZ} (red triangles). (e, f) Porod exponent m.
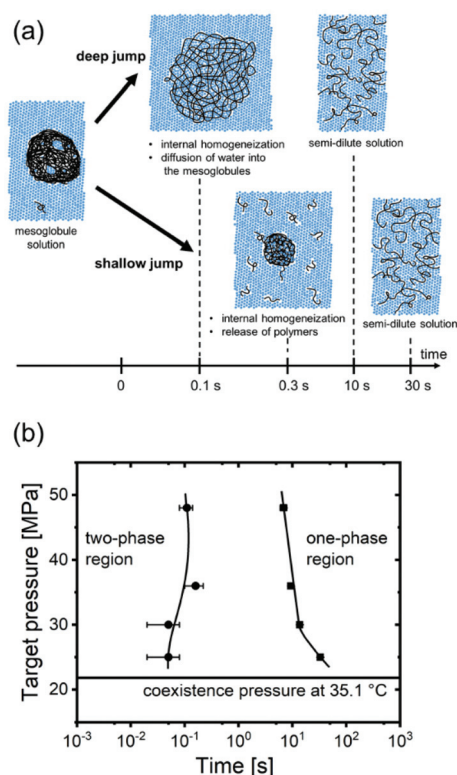
Fig. 4 (a) Schematic representation of the pathway of mesoglobule disintegration after a deep (top) and a shallow pressure jump (bottom). (b) Resulting time–pressure transformation diagram. The horizontal line denotes the coexistence pressure at 35.1 °C. Circles and squares mark the times identified for the start of the swelling of the mesoglobules and for the levelling off of the correlation length (Fig. S5 in the ESI†). The curved lines guide the eye.

for the shallowest jump. It is driven by the mechanism depicted in the top row of Fig. 4a: water diffuses into the mesoglobules, which makes them swell, as evident from the increased correlation length of the inner concentration fluctuations. This swelling process continues until a homogeneous semi-dilute solution is obtained.

Influence of target pressure. The results from two additional jumps having intermediate target pressures (30 and 36 MPa, for the results see Fig. S3 and S4 in the ESI†) confirm the findings discussed above: whereas for p_{target} = 25 MPa, R_g shrinks, it increases for 30–48 MPa. ξ_{OZ} decreases with time for 25 and 30 MPa, while it increases for 36 and 48 MPa, before the values become constant. At the end of the transformation, ξ_{OZ} reaches values which decrease from 17.6 to 11.0 nm for p_{target} increasing from 25 to 48 MPa. Thus, the deeper the target pressure is in the one-phase region, the more expanded is the chain conformation, *i.e.*, the better the solvent quality of water.[41]

To quantify the time scales in dependence on the target pressure, we construct a time-pressure transformation (TPT) diagram, in analogy to the well-known time-temperature transformation (TTT) diagrams that are used to characterize the time scales of phase transformations in dependence on temperature.[42] We extract the times when R_g starts to increase and when

ξ_{OZ} levels off (see arrows in Fig. S5 in the ESI†) and plot them in dependence on targe pressure (Fig. 4b). It is apparent that the transformation starts after 0.05–0.16 s, independent of p_{target}. The transition is close to completion after 33 s for p_{target} = 25 MPa, but earlier for the higher target pressures (7–14 s).

Thus, the target pressure—and correspondingly the magnitude of the osmotic pressure of the solvent inside the mesoglobules (or the solvent quality)—determines both the time scales and the disintegration mechanism of the mesoglobules. For target pressures close to the coexistence line, the low osmotic pressure of the surrounding water only permits weak swelling of the rigid outer layer. The mesoglobules decrease in size, because the disentanglement time of the chains at their surface is sufficiently short to allow the release of single chains. For larger differences of the target pressure from the coexistence line, the high osmotic pressure leads to a much faster diffusion of water into the mesoglobules, which is more rapid than the disentanglement processes. Here, the dominant mechanism of mesoglobule disintegration is the penetration of water into the mesoglobules across the rigid layer, leading to their continuous swelling.

Conclusions

The structural changes during the disintegration of polymeric nanoparticles are investigated with unprecedented temporal resolution (0.05 s) and over a large range of length scales (~1–100 nm). The transformation is initiated by pressure jumps from the two-phase region (dispersion of mesoglobules) to the one-phase region (semi-dilute solution) of an aqueous PNIPAM solution, while the kinetics are measured with small-angle neutron scattering. Starting from the same initial pressure, the target pressure was varied, which alters the osmotic pressure of the solvent. Two essential mechanisms are identified: for jumps deep into the one-phase region, the osmotic pressure of the solvent is sufficiently high to swell them. This is not the case for shallow jumps, where the release of single polymers dominates. Thus, by altering the target pressure, and, therefore, the osmotic pressure of the solvent, the mechanism by which mesoglobules disintegrate may be controlled.

These results are of key importance for the tuning of the switching process in applications of responsive polymers for transport and release purposes. The comparatively simple polymer PNIPAM serves as a model system for more complex biological macromolecules, such as cellulose or proteins.

Conflicts of interest

There are no conflicts to declare.

Acknowledgements
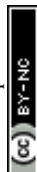
References

1 A. Parker, F. Vigoroux and W. F. Reed, *AIChE J.*, 2000, **46**, 1290.

2 A. Marabi, G. Mayor, A. Burbidge, R. Wallach and I. A. Saguy, *Chem. Eng. J.*, 2008, **139**, 118.

3 R. E. Martini, W. A. Brignole and S. E. Barbosa, *Polym. Eng. Sci.*, 2009, **49**, 602.

4 A. Dick Vethaak and J. Legler, *Science*, 2021, **371**, 672.

5 B. Narasimhan, *Adv. Drug Delivery Rev.*, 2001, **48**, 195.

6 E. Kaunisto, M. Marucci, P. Borgquist and A. Axelsson, *Int. J. Pharm.*, 2011, **418**, 54.

7 N. Kamaly, B. Yameen, J. Wu and O. C. Farokhzad, *Chem. Rev.*, 2016, **116**, 2602.

8 R. K. Saini, L. P. Bagri, A. K. Bajpai and A. Mishra, *Stimuli Responsive Polymeric Nanocarriers for Drug Delivery Applications*, 2018, vol. 1, p. 289.

9 Y. Fu and W. J. Kao, *Expert Opin. Drug Delivery*, 2019, **7**, 429.

10 B. A. Miller-Chou and J. L. Koenig, *Prog. Polym. Sci.*, 2003, **28**, 1223.

11 B. Medronho and B. Lindman, *Curr. Opin. Colloid Interface Sci.*, 2014, **19**, 32.

12 T. Budtova and P. Navard, *Cellulose*, 2016, **23**, 5.

13 A. Mogk, B. Bukau and H. H. Kampinga, *Mol. Cell*, 2018, **69**, 214.

14 N. B. Nillegoda, A. S. Wentink and B. Bukau, *Trends Biochem. Sci.*, 2018, **43**, 285.

15 B. Narasimhan and N. A. Peppas, *J. Pharm. Sci.*, 1997, **86**, 297.

16 T. Ribar, R. Bhargava and J. L. Koenig, *Macromolecules*, 2000, **33**, 8842.

17 P. Valois, E. Verneuil, F. Lequeux and L. Talini, *Soft Matter*, 2016, **12**, 8143.

18 V. Marcon and N. F. A. van der Vegt, *Soft Matter*, 2014, **10**, 9059.

19 P. Valois, E. Verneuil, F. Lequeux and L. Talini, *Soft Matter*, 2016, **12**, 8143.

20 A. Halperin, M. Kröger and F. M. Winnik, *Angew. Chem., Int. Ed.*, 2015, **54**, 15342.

21 Y. Maeda, T. Higuchi and I. Ikeda, *Langmuir*, 2000, **16**, 7503.

22 N. Osaka, M. Shibayama, T. Kikuchi and O. Yamamuro, *J. Phys. Chem. B*, 2009, **113**, 12870.

23 S. A. Deshmukh, S. K. R. S. Sankaranarayanan, K. Suthar and D. C. Mancini, *J. Phys. Chem. B*, 2012, **116**, 2651.

24 B.-J. Niebuur, W. Lohstroh, M.-S. Appavou, A. Schulte and C. M. Papadakis, *Macromolecules*, 2019, **52**, 1942.

25 C. Wu and X. Wang, *Phys. Rev. Lett.*, 1998, **80**, 4092.

26 Y. Okada and F. Tanaka, *Macromolecules*, 2005, **38**, 4465.

27 V. Aseyev, S. Hietala, A. Laukkanen, M. Nuopponen, O. Confortini, F. E. Du Prez and H. Tenhu, *Polymer*, 2005, **46**, 7118.

28 P. Kujawa, V. Aseyev, H. Tenhu and F. M. Winnik, *Macromolecules*, 2006, **39**, 7686.

29 E. A. Maresov and A. N. Semenov, *Macromolecules*, 2008, **41**, 9439.

30 B.-J. Niebuur, K.-L. Claude, S. Pinzek, C. Cariker, K. N. Raftopoulos, V. Pipich, M.-S. Appavou, A. Schulte and C. M. Papadakis, *ACS Macro Lett.*, 2017, **6**, 1180.

31 Y. Chen and S. Sajjadi, *Colloid Polym. Sci.*, 2014, **292**, 1319.

32 B.-J. Niebuur, L. Chiappisi, X. Zhang, F. Jung, A. Schulte and C. M. Papadakis, *ACS Macro Lett.*, 2018, **7**, 1155.

33 B.-J. Niebuur, L. Chiappisi, F. Jung, X. Zhang, A. Schulte and C. M. Papadakis, *Macromolecules*, 2019, **52**, 6416.

34 B. A. Hammouda, *J. Appl. Crystallogr.*, 2010, **43**, 716.

35 J. T. Koberstein, B. Morra and R. S. Stein, *J. Appl. Crystallogr.*, 1980, **13**, 34.

36 S. Ciccariello, *J. Appl. Crystallogr.*, 1988, **21**, 117.

37 M. Shibayama, T. Tanaka and C. C. Han, *J. Chem. Phys.*, 1992, **97**, 6829.

38 G. Porod, *Kolloidn. Zh.*, 1951, **124**, 83.

39 N. A. Peppas, J. C. Wu and E. D. von Meerwall, *Macromolecules*, 1994, **27**, 5626.

40 A. Körner, A. Larsson, L. Piculell and B. Wittgren, *J. Phys. Chem. B*, 2005, **109**, 11530.

41 M. Shibayama, T. Tanaka and C. C. Han, *J. Chem. Phys.*, 1992, **97**, 6842.

42 S. Lee, C. Leighton and F. S. Bates, *Proc. Natl. Acad. Sci. U. S. A.*, 2014, **111**, 17723.